Materials Letters 63 (2009) 2249–2252

Contents lists available at ScienceDirect

Materials Letters

journal homepage: www.elsevier.com/locate/matlet

Building desired heterojunctions of semiconductor CdS nanowire and carbon nanotube via AAO template-based approach

Fangming Han, Guowen Meng *, Xianglong Zhao, Qiaoling Xu, Jianxiong Liu, Bensong Chen, Xiaoguang Zhu, Mingguang Kong

Key Laboratory of Materials Physics, and Anhui Key Laboratory of Nanomaterials and Nanostructures, Institute of Solid State Physics, Chinese Academy of Sciences, Hefei 230031, People's Republic of China

ARTICLE INFO

Article history:
Received 11 May 2009
Accepted 22 July 2009
Available online 29 July 2009

Keywords:
Heterojunction
CdS nanowire
Carbon nanotube
Electronic transport

ABSTRACT

Heterojunctions of CdS nanowire (CdSNW) and carbon nanotube (CNT) have been achieved in the nanochannels of anodic aluminum oxide (AAO) templates via sequentially electrodepositing CdSNWs and chemical vapor depositing CNTs. Transport measurements reveal that Ohmic-like behavior has been achieved, which may result from a very low energy barrier in the junction of CdSNW/CNT. Furthermore, three-segment heterostructures of CNT/CdSNW/CNT have also been obtained by adding a procedure of selectively etching part of the deposited CdSNWs before chemical vapor depositing CNTs. The approach could be exploited to build nanodevices and functional networks consisting of well-interconnected two- or three-segment nanoheterostructures.

1. Introduction

Segmented heterojunctions consisting of one-dimensional (1D) nanostructures have attracted much attention due to their potential applications in electronic and photovoltaic devices, sensors, energy conversion and interconnection in integrate circuit [1–3]. Among the 1D segmented nanoheterojunctions, carbon nanotube (CNT)-based nanoheterojunctions have been extensively investigated for their potentials in nanoscale electronics and photoelectronics [4–6]. Up to now, CNT-based nanoheterojunctions of metal nanowire (MNW) and CNT (i.e., MNW/CNT) have been produced by a combination of electrodeposition (ED) and chemical vapor deposition (CVD) inside the nanochannels of anodic aluminum oxide (AAO) templates [7–9]. However, little is reported on the junctions consisting of CNT and semiconductor NW via AAO template-based approach. Although most CNT-based electronics nowadays are built with metallic contacts, CNT-based semiconductor/semiconductor heterojunctions could have a wide variety of applications [6]. Thus, building semiconductor NW and CNT heterojunctions with novel properties will be a great challenge.

CdS, as a direct wide band gap (2.42 eV) semiconductor in the visible region, has long been considered as a prime material for solar cells, electronics and optoelectronics nanodevices [10,11]. Here, we report the controlled synthesis of 1D segmented nanoheterojunctions of CdS NW (CdSNW) and CNT (i.e. CdSNW/CNT) and three-segment nanoheterostructures of CNT/CdSNW/CNT inside the nanochannels of AAO templates by a combination of electrodepositing CdSNWs, selective etching part of the NWs and CVD growth of CNTs [7,12]. The electrical properties were measured and the Ohmic-like behavior was confirmed in CdSNW/CNT nanojunctions.

2. Experimental

The experimental procedures for building two-segment CdSNW/CNT and three-segment CNT/CdSNW/CNT heterostructures are shown schematically in Fig. 1. The AAO templates were prepared by using a modified two-step anodization process as reported previously [13]. The CdSNW/CNT heterojunctions were achieved by first electrodepositing CdSNWs in the nanochannels of the AAO template with one side coated with a silver layer as electrode [14,15], and then growing CNTs in the remaining empty channels via CVD approach [13]. As for the three-segment CNT/CdSNW/CNT nanoheterostructures, the silver layer was etched using a concentrated HNO_3 solution after the ED of CdSNWs, and then a small portion of the CdSNWs near the planar surface side of the template was removed in a dilute HCl solution. Subsequently, CVD was carried out to deposit CNTs on the two empty sides of the nanochannels. The resultant products were placed into a plasma cleaner to remove the surface amorphous carbon. For scan electron microscope (SEM) and transmission electron microscope (TEM) characterizations, the nanoheterostructures were released from the AAO templates by dissolving the templates in a 3 M NaOH solution for 40 min at 50 °C, and then washed in distilled water for several times.

* Corresponding author. Tel.: +86 551 5592749; fax: +86 551 5591434.
E-mail address: gwmeng@issp.ac.cn (G. Meng).

0167-577X/$ – see front matter © 2009 Elsevier B.V. All rights reserved.
doi:10.1016/j.matlet.2009.07.044

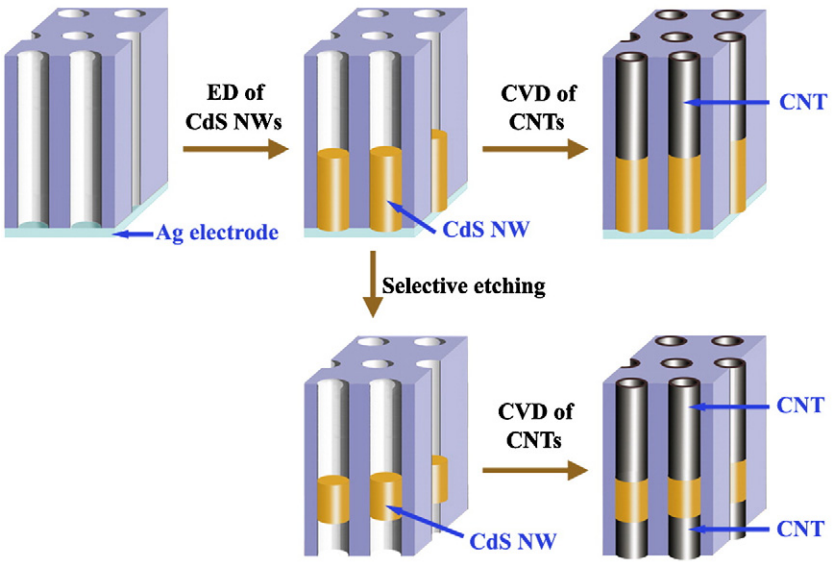

Fig. 1. Schematics for the fabrication procedure of two-segment CdSNW/CNT and three-segment CNT/CdSNW/CNT nanoheterostructures.

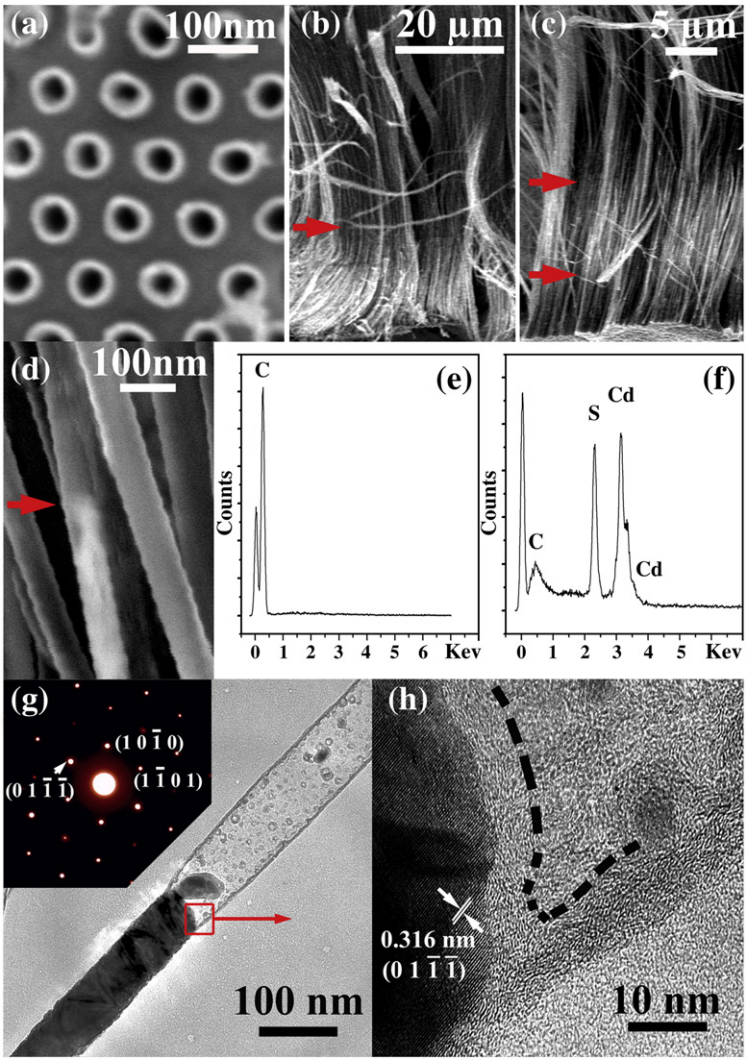

Fig. 2. Characterization of the nanoheterostructures. (a) Top view of the nanotube tip arrays. (b)–(d) SEM images of a bundle of CdSNW/CNT (b), CNT/CdSNW/CNT (c) heterostructures and an individual CdSNW/CNT nanoheterojunction (d), respectively, the interface of heterojunctions marked with red arrows. (e), (f) EDS spectra taken on the dark and light contrast parts in CdSNW/CNT and CNT/CdSNW/CNT heterostructures, respectively. (g) TEM image of an individual CdSNW/CNT heterojunction, with SAED pattern taken from CdSNW segment (inset). (h) Lattice-resolved TEM image showing the junction of CdSNW/CNT taken from the red rectangle in (g), the edge of the wall and tip of CNT is contoured by dashed black lines for clarity. (For interpretation of the references to color in this figure legend, the reader is referred to the web version of this article.)

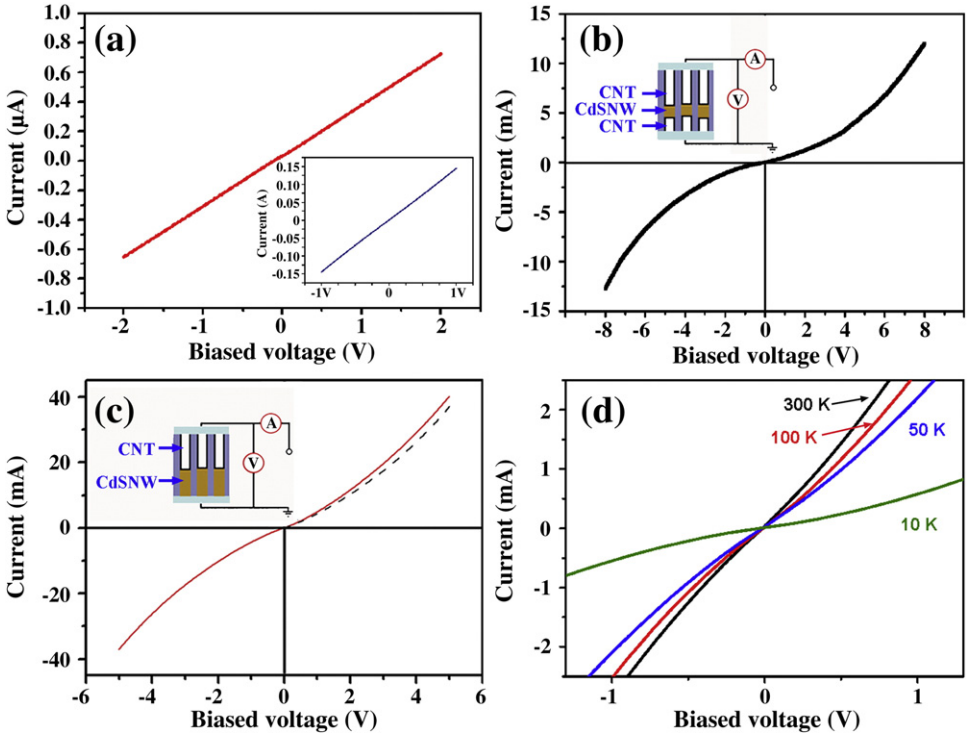

Fig. 3. (a) Room-temperature *I–V* characteristics of CdSNWs and CNTs (inset) embedded in AAO templates with both surface sides coated with silver layer as electrodes. (b), (c) Room-temperature *I–V* characteristics of CNT/CdSNW/CNT and CdSNW/CNT heterostructures, respectively. The black dashed line in (c) is the mirror image of the reverse current with regard to the origin. (d) *I–V* curves of CdSNW/CNT heterojunctions at different temperatures.

3. Results and discussion

Fig. 2a is the SEM image taken on the planar surface of the template embedded with the nanoheterojunctions, revealing the top view of the CNTs. Fig. 2b and c shows the SEM images of a bundle of CdSNW/CNT and CNT/CdSNW/CNT heterostructures, respectively. Close-up view (Fig. 2d) of the CdSNW/CNT heterojunctions clearly shows that the CNT and CdSNW are well connected, and both of the CNT and CdSNW segments are about 60 nm in diameter. Combined with energy dispersive X-ray spectroscopy (EDS) taken on the corresponding parts with different contrasts (Fig. 2e and f), it is confirmed that the light and dark contrast parts in Fig. 2b and c are CdSNWs and CNTs segments, respectively. The CNT segment appears darker than that of CdSNW due to its lower energy of the scattered electrons [16]. TEM image (Fig. 2g) of a single CdSNW/CNT junction further confirms that good connection between CdSNW and CNT has been achieved, and the selected area electron diffraction (SAED) pattern (inset in Fig. 2g), taken from the NW segment, shows that the NW is single crystal CdS with the hexagonal structure, partially resulted from the high temperature heating during the CNT growth. High-resolution TEM image of the CdSNW/CNT junction (Fig. 2h) shows that the CNT is closely ended at the CdSNW tip as CdSNW serves as a closely ended cap, and good adherence is achieved between the CdSNW and the CNT.

The electronic transport of the nanoheterostructures was examined. Prior to the measurements, thin silver layers were sputtered onto both planar surface sides of the AAO templates embedded with the resultant nanostructures to serve as working electrodes. First, we examined AAO templates embedded with only CdSNWs and CNTs respectively, and the electronic transport measurements show the linear and symmetrical *I–V* curves (Fig. 3a), revealing that both of the CdSNWs and CNTs could form Ohmic contacts with silver. Therefore, using similar measurement method, the resultant *I–V* curves will reveal the natural behavior of the heterostructures. Fig. 3b displays the room-temperature *I–V* curve of the CNT/CdSNW/CNT heterostructures with approximate symmetrical behavior, which is expected for the symmetrical configuration. Fig. 3c is the room-temperature *I–V* curve of the CdSNW/CNT heterojunctions, suggesting that Ohmic-like contacts are formed in the CdSNW/CNT junctions due to the approximate symmetrical behavior. However, the curve is not strictly symmetrical, and the forward current is higher than the reverse current (dashed) with the forward direction being positively biased CNTs. This might be attributed to a low energy barrier in the CdSNW/CNT junctions.

To understand the transport mechanism qualitatively, energy band diagram is displayed in Fig. 4, determined by the electron affinity and band gaps of the two materials. The electron affinity of the CNT is about 4.4 eV derived from the parameter of graphite [17], and the band gap energy (E_g) of 60-nm-diameter CNT is less than 0.10 eV derived from the equation $E_g \sim 1/D$ [18,19], where D is the diameter of the CNT. In this case, we assume that E_g is 0.10 eV and the Fermi level (Ef) of the CNT is in the middle of the band gap [17]. However, those parameters we introduced are not constants, which could be changed slightly with the diameter and the structure of the tips [20]. Also, the electron affinity of CdS is about 4.5 eV, and E_g of CdS is 2.42 eV [10].

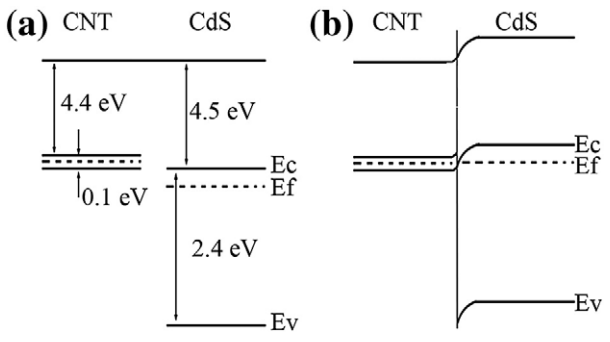

Fig. 4. Energy band diagrams of a CdSNW/CNT contact. (a) Before contact. (b) The proposed model of CdSNW/CNT after contact at thermal equilibrium.

After contacting, the electrons in CNTs move to CdSNW, then the conduction band of CdS bends to the downward at the transition region. Thus from Fig. 4b, one would expect to observe Ohmic-like behavior in the CdSNW/CNT nanojunctions. Furthermore, there could be a very low barrier at the interface to prevent the electrons from CNT moving to CdS.

The electronic transport properties from another sample at the temperature ranging from 10 K to 300 K are shown in Fig. 3d. At elevated temperatures the high current flow may be associated with increased electron excitation, thus generating more free carriers to participate in the conduction process. It should be emphasized that although the linear and symmetrical behavior approximately has been observed at 300 K, it is found that with the decrease of the temperature the *I–V* characteristic moves from linear to nonlinear. This could be attributed to the reduction of the barrier height at elevated temperatures, and which is a nonlinear function of ambient temperature [21].

4. Conclusions

In summary, we have fabricated two-segment CdSNW/CNT and three-segment CNT/CdSNW/CNT nanoheterostructures by a combination of ED of CdSNWs, selective etching part of the deposited CdS NWs, and CVD growth of CNTs inside the remaining nanochannels of the AAO templates. Electronic transport measurements reveal that the CdSNW/CNT heterojunctions show Ohmic-like behavior. The method reported here could be extended to build CNT-based two- and three-segment heterojunctions with the NW segment consisting of other semiconducting materials achievable via electrodeposition and stable at the CNTs growth temperature. These CNT-based heterojunctions may have potentials in nanoelectronics.

Acknowledgments

We thank financial supports from the National Natural Science Foundation of China (Grant No. 50525207 and 10374092), and National Basic Research Program of China (Grant No. 2007CB936601).

References

[1] Gudiksen MS, Lauhon LJ, Wang J, Smith DC, Lieber CM. Nature 2002;415:617–20.
[2] Kempa TJ, Tian BZ, Kim DR, Hu JS, Zheng XL, Lieber CM. Nano Lett 2008;8:3456–60.
[3] Guo YB, Tang QX, Liu HB, Zhang YJ, Li YL, Hu WP, Wang S, Zhu DB. J Am Chem Soc 2008;130:9198–9.
[4] Hu JT, Ouyang M, Yang PD, Lieber CM. Nature 1999;399:48–51.
[5] Zhang Y, Ichihashi T, Landree E, Nihey F, Iijima S. Science 1999;285:1719–22.
[6] Liang CW, Roth S. Nano Lett 2008;8:1809–12.
[7] Luo J, Zhang L, Zhang YJ, Zhu J. Adv Mater 2002;14:1413–4.
[8] Luo J, Huang ZP, Zhao YG, Zhang L, Zhu J. Adv Mater 2004;16:1512–5.
[9] Luo J, Xing YJ, Zhu J, Yu DP, Zhao YG, Zhang L, Fang H, Huang ZP, Xu J. Adv Funct Mater 2006;16:1081–5.
[10] Liu GM, Schulmeyer T, Brötz J, Klein A, Jaegermann W. Thin Solid Films 2003;431–432:477–82.
[11] Ma RM, Dai L, Huo HB, Xu WJ, Qin GG. Nano Lett 2007;7:3300–4.
[12] Ou FS, Shaijumon MM, Ci LJ, Benicewicz D, Vajtai R, Ajayan PM. Appl Phys Lett 2006;89:243112.
[13] Meng GW, Jung YJ, Cao AY, Vajtai R, Ajayan PM. Proc Natl Acad Sci USA 2005;102:7074–8.
[14] Routkevitch D, Bigioni T, Moskovits M, Xu JM. J Phys Chem 1996;100:14037–47.
[15] Xu DS, Xu YJ, Chen DP, Guo GL, Gui LL, Tang YQ. Chem Phys Lett 2000;325:340–4.
[16] Pena DJ, Mbindyo JKN, Carado AJ, Mallouk TE, Keating CD, Razavi B, Mayer TS. J Phys Chem B 2002;106:7458–62.
[17] Tzolov M, Chang B, Yin A, Straus D, Xu JM. Phys Rev Lett 2004;92:075505.
[18] Rakitin A, Papadopoulos C, Xu JM. Phys Rev B 2000;61:5793–6.
[19] Kuo TF, Tzolov MB, Straus DA, Xu J. Appl Phys Lett 2008;92:212107.
[20] Xu Z, Bai XD, Wang EG, Wang ZL. Appl Phys Lett 2005;87:163106.
[21] Ahmed MM, Karimov KhS, Moiz SA. IEEE T Electron Dev 2004;51:121–6.